Hindawi
International Journal of Photoenergy
Volume 2020, Article ID 8821687, 15 pages
https://doi.org/10.1155/2020/8821687

Research Article

Dynamic Heating System of Multiphase Flow Digester by Solar-Untreated Sewage Source Heat Pump

Pei Guo,[1] Jiri Zhou,[1] Rongjiang Ma,[2] Nanyang Yu ,[1] and Yanping Yuan[1]

[1]*School of Mechanical Engineering, Southwest Jiaotong University, Chengdu 610031, China*
[2]*Department of Building Science, Tsinghua University, Beijing 100084, China*

Correspondence should be addressed to Nanyang Yu; rhinos@126.com

Received 22 May 2020; Revised 17 June 2020; Accepted 10 July 2020; Published 3 August 2020

Academic Editor: Dhruba B. Khadka

The traditional biogas heating system has the disadvantages of a low energy efficiency ratio and high energy consumption. In this study, a solar-untreated sewage source heat pump system (SUSSHPS) was developed for heating a 12 m^3 multiphase flow digester (MFD) in Suining, China. To investigate the operating effects, two modes were defined according to the solar fractions in different regions. On the basis of experimental data, thermodynamic calculations and operating simulation analysis were performed, and the solar collector area (A_c) and the minimum length of the sewage double-pipe heat exchanger (l_{min}) for the two modes were calculated. The results indicated that the A_c and l_{min} of mode 2 were larger than those of mode 1 at different solar fractions. Additionally, the results suggested that mode 1 can be used at a solar fraction of <0.33, and mode 2 can be used at a solar fraction of >0.5. Moreover, a comprehensive evaluation of different biogas heating systems was performed. Two evaluation methods were used for modeling calculations, and the results of the two methods were consistent. The SUSSHPS had the largest comprehensive evaluation value among the four systems. The proposed SUSSHPS can play a significant role in improving current biogas heating systems and promoting the development of biogas projects.

1. Introduction

Biogas is a renewable form of energy that is produced by the anaerobic digestion of organic waste at a certain temperature, pH, and concentration [1]. Temperature is one of the factors affecting anaerobic digestion. The temperature variation significantly affects the bacterial digestion process and therefore should not exceed 2–3°C per hour [2]. If the variation in the digestion temperature exceeds 5°C within a short period of time, the biogas production rate can change significantly; thus, a constant digestion temperature is required [3]. Therefore, it is generally accepted that the current biogas project should be equipped with a heating system to ensure stable biogas production during winter.

Traditional heating methods include generation waste heat heating [4], boiler heating [5, 6], active and passive solar heating [7, 8], and heat pump heating [9]. Liu et al. used a groundwater source heat pump to heat a 700 m^3 anaerobic digester and found that the fermentation temperature of biogas tanks could be maintained at 33–35°C in winter [10]. Tiwari et al. used a photovoltaic thermal-integrated greenhouse system for biogas heating, and simulation results indicated that the greenhouse room temperature varied between 38 and 47°C [11]. In recent years, for reducing the active energy input and avoiding the high initial cost and unstable defects in the use of single solar energy, solar-integrated source heat pump heating methods have become a popular research topic [12]. These methods include solar-ground source heat pump heating [13], solar-air source heat pump heating [14], and solar-sewage source heat pump heating [15]. However, solar-integrated source heat pump heating methods have many disadvantages, limiting their applications. First, the heating system has a low energy efficiency ratio (EER). Pei et al. used a solar-ground source heat pump to heat a 69.3 m^3 anaerobic digester, and the system EER was 2.7 [16]. Another disadvantage of the solar-ground source heat pump heating method is the reduction of the EER over time, which is due to the heat storage imbalance in winter and summer [17]. The disadvantage of the solar-air source heat pump heating method is frosting in winter [18]. Solar-

Table 1: Comparison of different biogas heating systems.

Heating system	Digestion temperature (°C)	CH_4 yield ($m^3\ m^{-3}\ d^{-1}$)	System unit cost* (yuan m^{-3})	EER	Reference
Electric boiler	23.5	0.472	/	1.38	[20]
Biogas boiler	35	0.482	2000	1.01	[19]
Solar+biogas boiler	19.82-23.5	0.389-0.472	314.39	2.01	[6]
Solar direct heating system	26-37	0.63-1.08	2145.16	6.17	[7]
Solar direct heating system	7.02-27.14	0.314-0.569	300	5.56	[21]
Ground source heat pump	32	0.6	408.37	2.7	[9]
Solar-air source heat pump	35	/	3750	3	[14]

*The value is the system initial cost divided by the volume of the digester.

sewage source heat pump heating is different from the other two methods and has the advantages of a higher EER, a lower initial cost, and easy maintenance. However, the corrosion and blockage of the heat exchangers are significant problems affecting the system application. Additionally, the system is limited to using the primary or secondary water discharged from a sewage treatment plant as a heat source. A comparison of the different biogas heating systems is presented in Table 1.

As shown in Figure 1, a 12 m^3 multiphase flow digester (MFD) dynamic digestion system was heated by a biogas boiler near a pig farm at Suining City, Sichuan Province, China [19]. Full-scale field experiments were conducted on the biogas production rate of the system at different temperatures, as well as the dynamic digestion effects and dynamic heating digestion effects of the system. The results for the biogas production rate at different temperatures revealed that the temperature significantly affected the biogas production rate of the MFD system. After long-term operation, although the biogas boiler system had the advantages of convenient operation and easy maintenance, the high energy consumption and low EER reduced the overall efficiency of the biogas project, making it difficult to maintain stable long-term operation.

Accordingly, an integrated solar-untreated sewage source heat pump dynamic heating system for the MFD was developed in this study. A predesigned double-pipe device was used as the heat exchanger, which extracts thermal energy from untreated sewage. The structure of the device avoids the problems of corrosion and blockage, expanding the application scope of the heating system. Additionally, the system does not affect the biochemical treatment of sewage [22]. Furthermore, two operating modes were designed according to the solar fractions in different regions. Through thermodynamic calculations and operating simulation analysis, the variation of the solar collector area (A_c) and the minimum length of the sewage double-pipe heat exchanger (l_{min}) under the two operating modes were obtained, and the application ranges of the operation modes were determined. To quantitatively compare the advantages of the solar-untreated sewage source heat pump system (SUSSHPS) over different heating systems, a comprehensive evaluation of different biogas heating systems was conducted, and calculations were performed using two methods. This study may help promote the use of the integrated solar-untreated sewage source heat pump in the biogas heating field and lead to developments in biogas science research. Moreover, this study can increase the biogas production rate and maintain the stability of biogas projects in winter.

2. System Descriptions and Methods

2.1. System Descriptions. The proposed system (Figure 2) contains two subsystems: the SUSSHPS and the biogas slurry dynamic heating and heat storage system. The SUSSHPS consists of a solar collector, a heat pump unit, a sewage double-pipe heat exchanger, and water pumps. The sewage double-pipe heat exchanger (Figure 3) is a part of the sewage network. Untreated sewage flows in the inner pipe, and chilled water flows in the spiral space between the inner and outer pipes. The thermal energy of the untreated sewage is transferred to the chilled water through the inner pipe wall, which then flows downstream after the heat exchange. Moreover, the solar collectors provide a portion of the heat. Then, the chilled water is pumped into the heat pump unit, and after heat exchange, it is pumped into the sewage double-pipe heat exchanger again. After transmission and conversion by the heat pump unit, thermal energy is transferred to the biogas slurry dynamic heating and heat storage system through the cooling water pump. In the biogas slurry dynamic heating and heat storage system, thermal energy is transferred to the slurry through the slurry double-pipe heat exchanger, and the excess heat is stored in the heat storage tank.

A heat pump unit is used in the system as the heat source for heating. The rated power, rated coefficient of performance (COP), and voltage of the heat pump unit were 1 kW, 4.0, and 380 kV, respectively. To reduce the power of the heat pump unit, a heat storage tank was used. The volume, length, width, and height of the tank were 2 m^3, 1.0 m, 1.0 m, and 2.0 m, respectively. The storage temperature was set as 313.15 K. The rated power, rated flow, head, and rotating speed of the chilled water pump and cooling water pump were 0.75 kW, 7 $m^3\ h^{-1}$, 12.5 m, and 2000 rpm, respectively.

2.2. Experimental Methods. The digestion material of the MFD is fresh pig manure. The detailed parameters of the MFD dynamic anaerobic digestion system are presented in [2]. Continuous feeding digestion experiments (450 kg per day) were started on February 22, 2016, and performed until

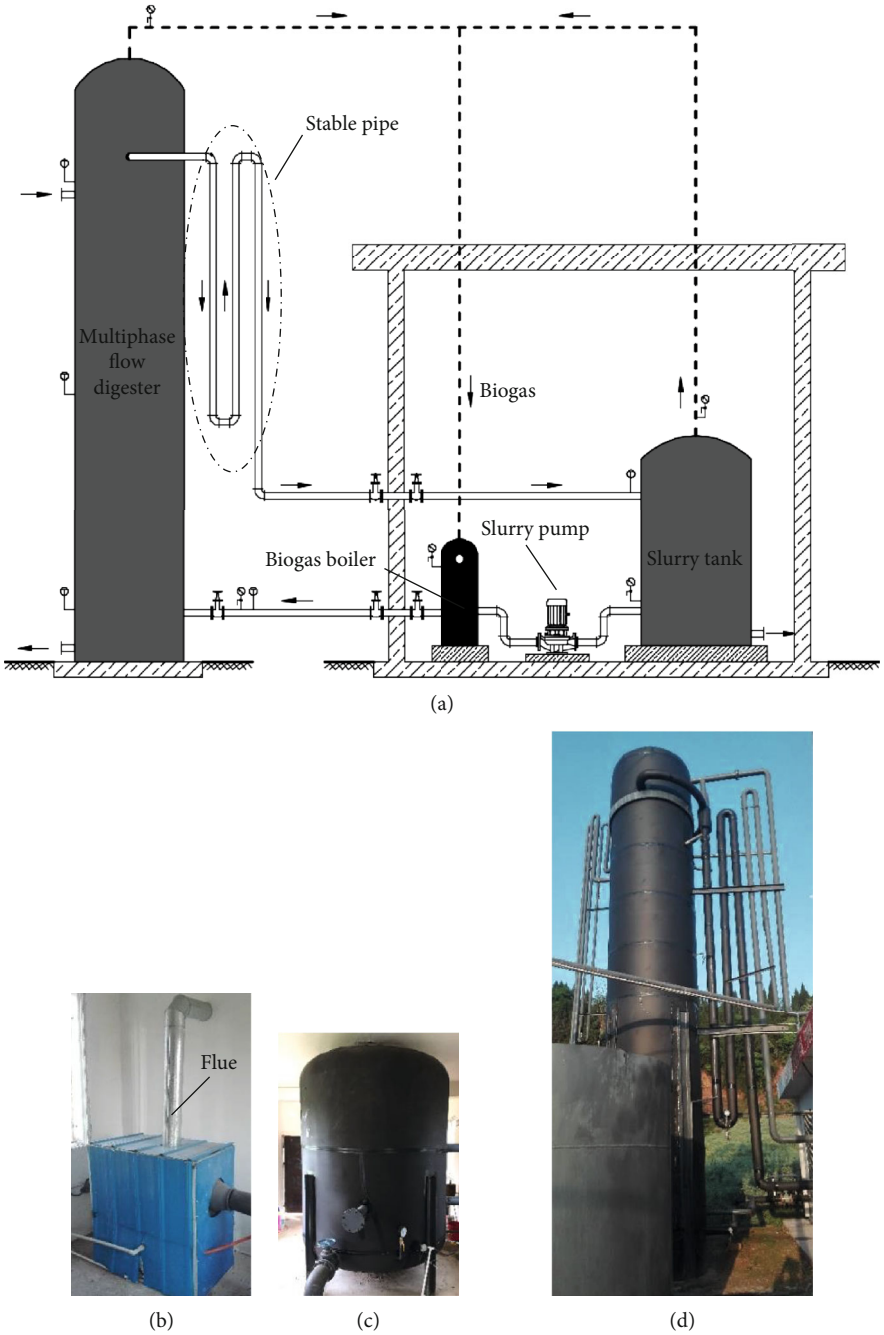

Figure 1: The anaerobic digestion system: (a) schematic diagram of multiphase flow digestion system; (b) image of biogas boiler; (c) image of slurry tank; (d) image of multiphase flow digester.

April 20, 2016. The basic characteristics of the biogas slurry used in the experiments are presented in Table 2.

The main measurement parameters include the digestion temperature, pump flow rate, storage temperature, and biogas production, as shown in Table 3.

2.3. System Operating Modes. Figure 4 presents the operating schematic of the SUSSHPS. As shown in Table 4 and Figure 5, the distribution of solar energy resources differs among different regions in Sichuan Province. Under different solar fractions, the necessary thermal energy supplied by the untreated sewage (Q_{sewage}) and solar energy (Q_{solar}) differs. Therefore, the system employs two operating modes. In mode 1, during the daytime, the thermal energy of the MFD dynamic heating and the heat storage tank are supplied by the SUSSHPS (①+②→③+④). At night, the thermal energy of the MFD dynamic heating is supplied by the SUSSHPS and the heat storage tank (①→④,⑤). In mode 2, during the daytime, the thermal energy of the MFD dynamic heating and the heat storage tank are supplied by the SUSSHPS (①+②→③+④). At night, the thermal energy of the MFD dynamic heating is supplied by the heat storage

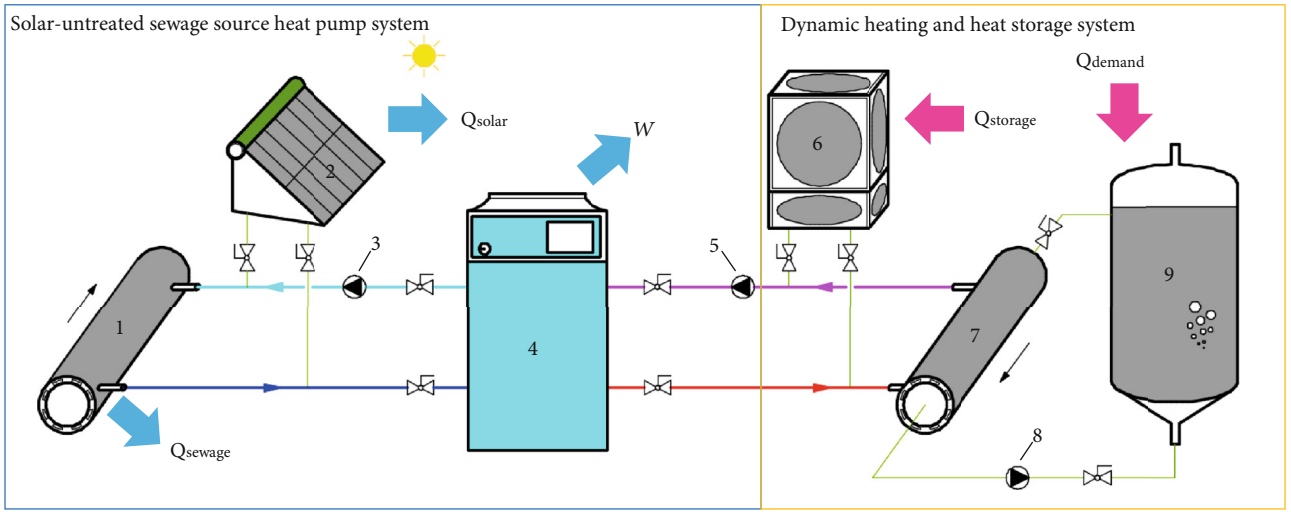

Figure 2: Schematic of the SUSSHPS and dynamic heating and heat storage system. 1—sewage double-pipe heat exchanger; 2—solar collector; 3—chilled water pump; 4—heat pump unit; 5—cooling water pump; 6—heat storage tank; 7—slurry double-pipe heat exchanger; 8—biogas slurry pump; 9—MFD.

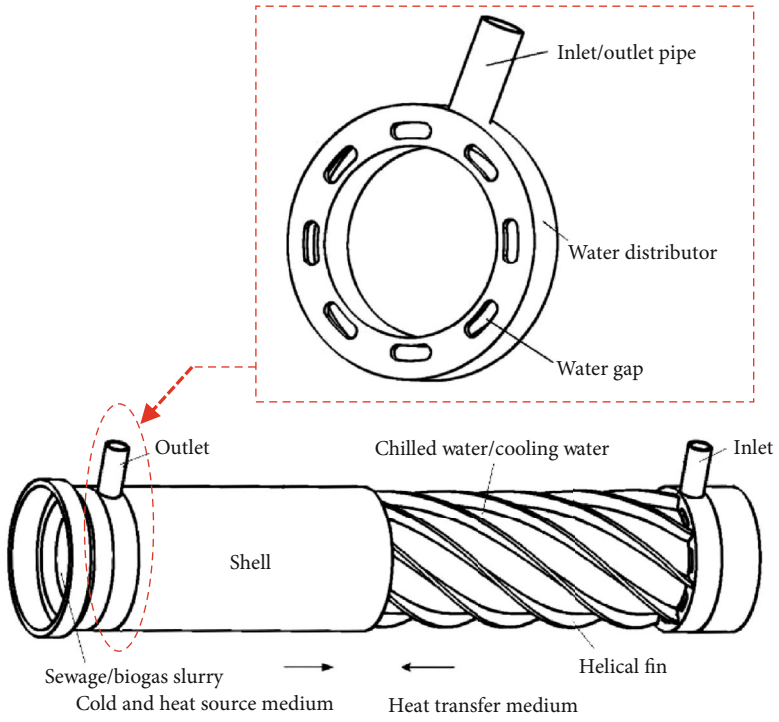

Figure 3: Schematic of the double-pipe heat exchanger.

Table 2: Characteristics of the biogas slurry.

Digestion temperature (°C)	pH	COD ($g\,L^{-1}$)	BOD_5 ($g\,L^{-1}$)	TS (%)	VS (%)
35	7.6	6537	3218	3.22	62.6

tank directly (⑤). To save energy, the heating system runs three times each day and night, for one hour each time. The heat transfer processes for the two modes are shown in Figures 6 and 7.

Similarly, the minimum length of the sewage double-pipe heat exchanger and the solar collector area are different for the two modes. The system heat load includes the heat loss of the slurry tank and the MFD and the heat load of the slurry, which must be heated to reach the target digestion temperature. Ignoring the bioheat and the heat removed by biogas, the system total heat demand can be described as follows [24].

$$Q_{demand} = Q_1 + Q_2, \quad (1)$$

Table 3: Characteristics of the measuring instrument.

Measurement parameter	Model	Manufacturer	Measurement range	Measurement precision	Manufacturing destination
Digestion temperature	pt100	Hangzhou Meikong Technology Co., Ltd.	-70 to 500°C	±0.1°C	Hangzhou, China
Sewage temperature	176 T3	Testo SE & Co., Ltd.	-195 to 1000°C	±0.1°C	Hamburg, Germany
Biogas production	SC300 G4	Chongqing Shancheng Gas Equipment Co., Ltd.	0-100 $m^3 h^{-1}$	±0.01 $m^3 h^{-1}$	Chongqing, China
Storage temperature	ZNHW-II	Henan Aibote Technology Co., Ltd	0-400°C	±0.1 °C	Henan, China
Pump flow rate	EMFM-HFD3000	Chengdu Youlide Instrument Co., Ltd.	0-100 $m^3 h^{-1}$	±0.01 $m^3 h^{-1}$	Chengdu, China

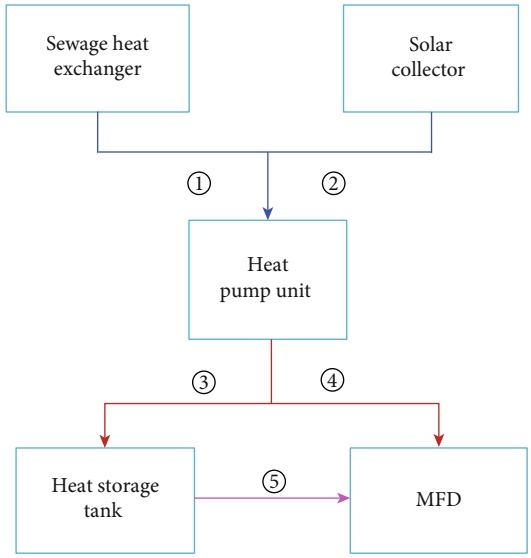

Figure 4: Operating schematic of the SUSSHPS.

Table 4: Recommended data for the solar fractions in Sichuan Province.

Resource division	Rank	Solar fraction
Solar energy resource-rich areas	I	>70%
Solar energy resource-rich areas	II	50%~70%
General-solar energy resource areas	III	30%~50%
Solar energy resource-poor areas	IV	10%~30%

where Q_{demand} represents the heat duty of the dynamic anaerobic digestion system (in kW), Q_1 represents the heat required for heating the biomass digestive fluid (in kW), and Q_2 represents the heat loss from the MFD and slurry tank (in kW). The specific calculation process is described in [19].

$$\begin{cases} 12Q_{demand} + Q_{storage} = 3W + 3Q_{sewage} + 3Q_{solar}, \\ 12Q_{demand} - Q_{storage} = 3W + 3Q_{sewage}, \end{cases} \quad (2)$$

$$\begin{cases} Q_{sewage} = (4Q_{demand} - W) \times (1 - f), \\ Q_{solar} = (8Q_{demand} - 2W) \times f. \end{cases} \quad (3)$$

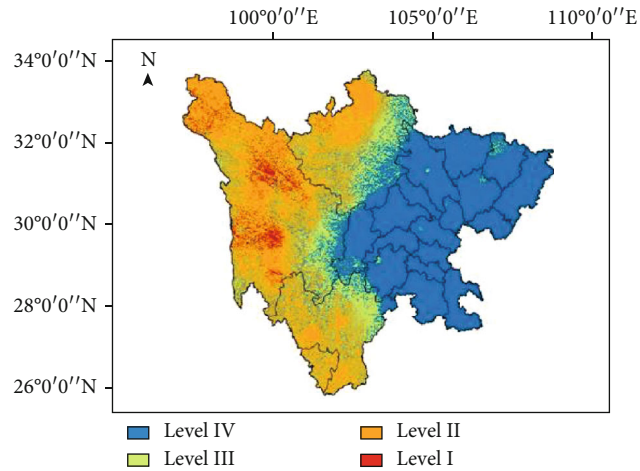

Figure 5: Distribution of solar energy richness in Sichuan [23].

$$\begin{cases} 12Q_{demand} + Q_{storage} = 3W + 3Q_{sewage} + 3Q_{solar}, \\ 12Q_{demand} = Q_{storage}, \end{cases} \quad (4)$$

$$\begin{cases} Q_{sewage} = (8Q_{demand} - W) \times (1 - f), \\ Q_{solar} = (8Q_{demand} - W) \times f. \end{cases} \quad (5)$$

Comparing Equation (3) with Equation (5) reveals that the thermal energy supplied by the untreated sewage and the solar irradiation in mode 1 are larger than those in mode 2, indicating that A_c and l_{min} for mode 1 are larger than those for mode 2.

2.3.1. Minimum Length of Sewage Double-Pipe Heat Exchanger. Figure 8 presents the measured and calculated [25] untreated sewage temperatures in winter in Suining City. As shown, the temperature of the untreated sewage was 13.4–16.2°C in winter, and the temperature fluctuation was small. Therefore, it is assumed that the sewage temperature was constant at 15°C.

As shown in Figure 2, the water–water heat transfer in the converse direction is kept in the heat exchanger. The flow of sewage in the inner pipe is natural convection, while the flow of chilled water in the outer pipe is forced convection. The l_{min} can be expressed as follows [26]:

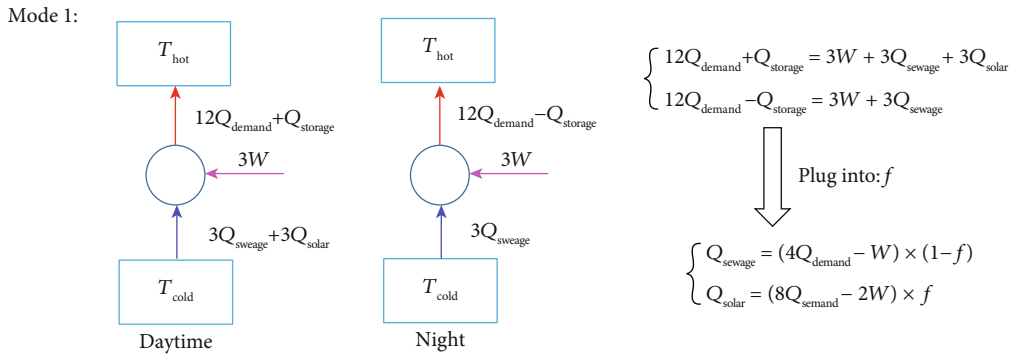

Figure 6: Heat transfer process of mode 1.

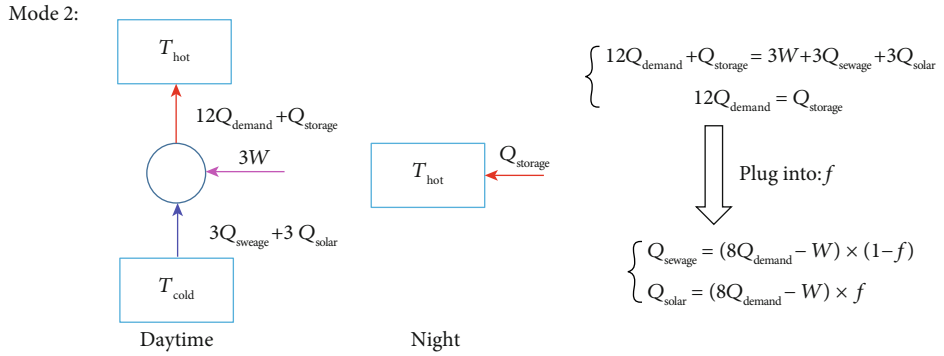

Figure 7: Heat transfer process of mode 2.

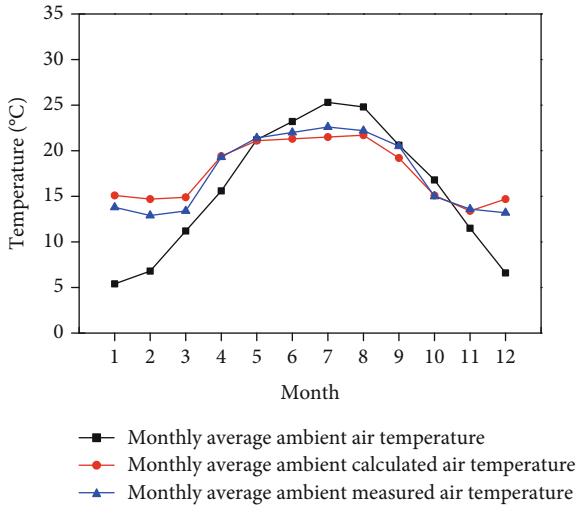

Figure 8: Comparison of the domestic sewage and outdoor monthly mean temperatures in Suining.

$$l = \frac{1000Q_{\text{sewage}} \cdot \ln\left(\left(t_{\text{sewage}} - t_{\text{in}}\right)/\left(\pi t_{\text{sewage}} - t_{\text{out}}\right)\right)}{k_{\text{m}} \cdot \left[\left(t_{\text{sewage}} - t_{\text{in}}\right) - \left(t_{\text{sewage}} - t_{\text{out}}\right)\right]}, \quad (6)$$

$$k_{\text{m}} = \frac{1}{R_{\text{I}} + (1/2\pi r_0 h_0)}, \quad (7)$$

$$h_0 = \frac{Nu \cdot \lambda_0}{D_{\text{e}}}, \quad (8)$$

$$D_{\text{e}} = 2r_{\text{o}} - 2r_{\text{i}} - 2\delta_{\text{o}} - 2\delta_{\text{i}}, \quad (9)$$

where $l_{\min}$ represents the minimum length of the sewage double-pipe heat exchanger (in m); t_{sewage} represents the calculation temperature of the sewage in winter (in K); t_{in} and t_{out} represent the average inlet and outlet temperatures of the chilled water, respectively (in K); k_{m} is the heat transfer coefficient of the heat exchanger (in W m^{-1} K^{-1}); R_{I} represents the fouling resistance, which is chosen as 0.00017 m K W^{-1} [27]; h_0 is the convection heat transfer coefficient of the inner pipe internal surface (in W m^{-2} K^{-1}); r_{i} represents the inner pipe radius of the sewage double-pipe heat exchanger (in m); r_0 represents the outer pipe radius of the double-pipe heat exchanger (in m); δ_{i} represents the thickness of the inner pipe wall (in m); δ_0 represents the thickness of the outer pipe wall (in m); λ_0 represents the heat conductivity coefficient of the chilled water (in W m^{-1} K^{-1}); Nu is the Nusselt criterion number; and D_{e} represents the characteristic length of the sewage double-pipe heat exchanger (in m). The values of the parameters used in the calculation are presented in Table 5.

2.3.2. Solar Collector Area. After Q_{demand} is determined, the solar collector area can be calculated for a specific solar fraction. A direct system was chosen, and A_{c} can be expressed as follows [28]:

$$Q_{\text{c}} = 86.4(1 + \eta_{\text{s}})Q_{\text{solar}},$$
$$A_{\text{c}} = Q_{\text{c}} \times \frac{f}{J_{\text{T}} \times \eta_{\text{d}} \times \left(1 - \eta_{\text{g}}\right)}, \quad (10)$$

Table 5: Basic values of the parameters for the sewage double-pipe heat exchanger.

Parameter	Unit	Value
Inner pipe radius	mm	23
Outer pipe radius	mm	39
Thickness of inner pipe wall	mm	2
Thickness of outer pipe wall	mm	3
Average inlet/outlet temperature of chilled water	K	280.15/285.15

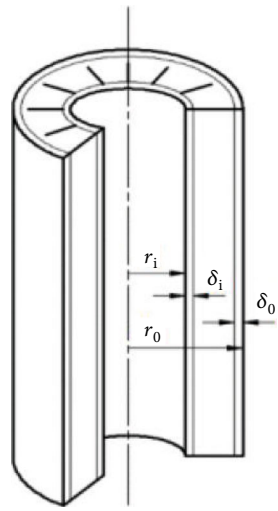

where A_c represents the area of the direct system (in m^2); f represents the solar fraction, as shown in Table 3; J_T represents the average daily amount of solar radiation ($6.82\,MJ\,m^{-2}\,d^{-1}$) [23]; η_d represents the average collection efficiency of the solar collector (0.25–0.50; chosen as 0.4 in this study); η_g represents the average heat loss rate of the solar collector (0.20–0.30; chosen as 0.2 in this study); η_s represents the heat loss efficiency of the direct system (chosen as 0.05); and Q_c represents the heat duty of the solar collector (in $MJ\,d^{-1}$).

3. Results and Discussion

The proposed SUSSHPS was designed to maintain dynamic anaerobic digestion at 35°C in winter. As indicated by Equation (6), the minimum length of the sewage double-pipe heat exchanger was determined by the heat transfer coefficients of the heat exchanger. Theoretical calculations and a numerical simulation analysis of the heat transfer coefficients of the heat exchanger were performed. As shown in Figure 9, the extended calculated values of the Dittus–Boelter equation and Gnielinski equation [29] were compared with the simulation value obtained using the ANSYS 15.0 software. The results indicated that the differences among the three numerical values were small, and the simulation results were accurate. Therefore, according to Equations (7)–(9), the calculated value of k_m was $292.43\,W\,m^{-1}\,K^{-1}$. Figure 10 presents the annual heat duty and heat loss of the SUSSHPS. Q_{demand} was calculated as 1.01 kW.

Table 6 presents the minimum length of the sewage double-pipe heat exchanger and the solar collector area under the different solar fractions in different modes. As shown, for both modes, with an increase in the solar fraction, the minimum length of the sewage double-pipe heat exchanger decreased, and the solar collector area increased. As shown in Figure 11, with a 0.1 m decrease of the minimum length of the sewage double-pipe heat exchanger, the increases in the solar collector area for modes 1 and 2 were 12.39 m^2 and 6.19 m^2, respectively. Consequently, the functional relationship between A_c and l_{min} can be expressed as follows: Mode 1: $Y = 252.76 - 123.86X$ ($R^2 = 0.9996$, $P < 0.0001$). Mode 2: $Y = 294.03 - 61.87X$ ($R^2 = 0.9996$, $P < 0.0001$).

The application conditions of the two modes were investigated. Mode 1 can be used in general-solar energy resource areas, where the amount of thermal energy supplied by the untreated sewage is larger than that supplied by the solar irradiation for the SUSSHPS. Conversely, mode 2 can be used in solar energy resource-rich areas, where the amount of thermal energy supplied by the untreated sewage was smaller than that supplied by the solar irradiation for the SUSSHPS. According to Equations (3) and (5), when $Q_{sewage} = Q_{solar}$, the solar fractions for modes 1 and 2 are 0.33 and 0.5, respectively. Thus, as shown in Figure 12, the standard deviations are 359.85 m (model 1) and 178.44 m (model 2) for Figure 12(a), and the standard deviations are 34.61 m^{-2} (model 1) and 40.23 m^{-2} (model 2) for Figure 12(b), when the solar fraction is <0.33, mode 1 is more suitable, and when the solar fraction is >0.5, mode 2 is more suitable. Additionally, it was useful to regulate the anaerobic digestion temperature when the solar fraction was between 0.33 and 0.5.

The simulation results were verified. A solar fraction of 0.3 and mode 1 were selected. Figure 13 presents the slurry temperature of the MFD from February 22, 2016, to April 10, 2016. As shown in Figure 13, the slurry temperature was stabilized around 35°C, indicating that the SUSSHPS functioned well and that stable digestion was achieved by the MFD.

4. Evaluation of System Operation

4.1. Establishment of Comprehensive Evaluation System. To examine the advantages of the SUSSHPS, a comprehensive evaluation of different biogas heating systems

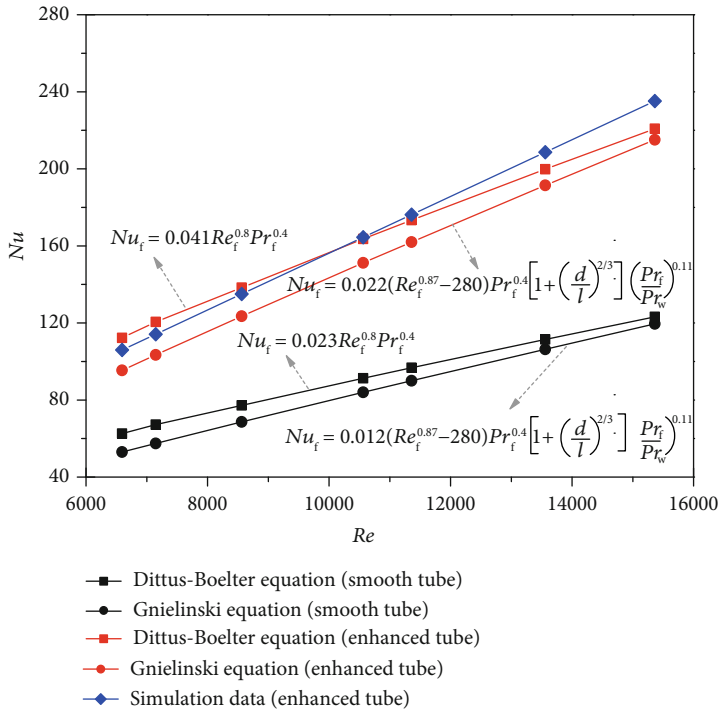

Figure 9: Comparison of Nu between the simulation data and empirical data.

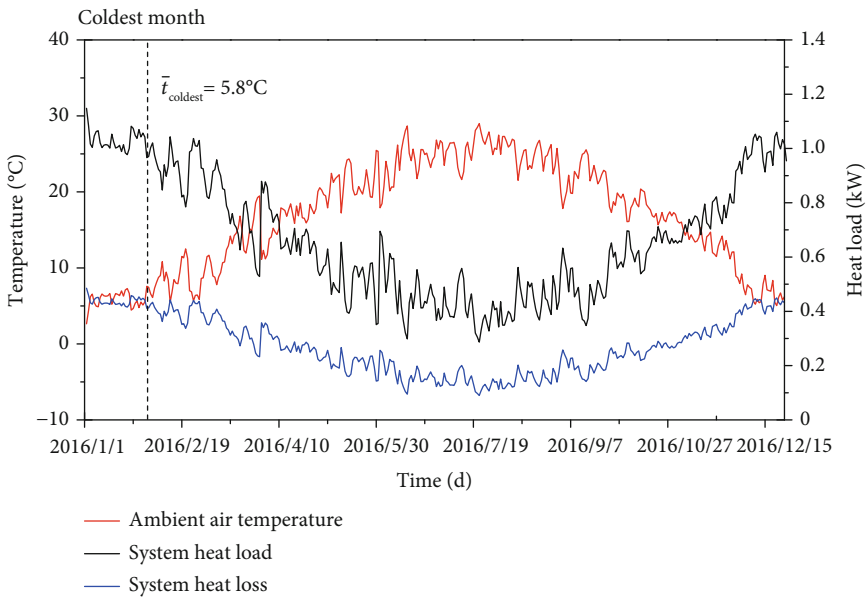

Figure 10: Annual heat duty and heat loss of the SUSSHPS.

was performed. The original biogas boiler heating system was labeled as "system 1," the solar direct heating system was labeled as "system 2," the solar source heat pump heating system was labeled as "system 3," the SUSSHPS with $l = l_{max}$ was labeled as "system 4," and the SUSSHPS with $l = l_{min}$ was labeled as "system 5."

Single-calculation analysis methods and software simulation analysis methods have been used in many system-evaluation studies [30]. However, these methods have many disadvantages. The problem of the single-calculation analysis methods affects the comprehensive evaluation of systems, as only the energy saving or economy of the system is considered [31]. The software simulation process simplifies the model indicators, which can cause calculation deviations [32]. Therefore, to evaluate each system quantitatively, a comprehensive evaluation system and a comprehensive evaluation mathematical model based on previous experimental data were constructed. According to the construction

Table 6: Minimum length of the sewage double-pipe heat exchanger and the solar collector area under the different solar fractions in different modes.

f	Mode 1		Mode 2	
	l_{min} (m)	A_c (m^2)	l_{min} (m)	A_c (m^2)
0.1	1.84	25.27	4.27	29.43
0.2	1.63	50.55	3.80	59.86
0.3	1.43	75.82	3.32	88.29
0.4	1.22	101.1	2.85	117.72
0.5	1.02	126.37	2.37	147.15
0.6	0.82	151.64	1.90	176.58
0.7	0.61	176.92	1.42	206.02
0.8	0.41	202.19	0.95	235.45
0.9	0.20	227.47	0.47	264.88
Standard deviation	0.56	69.22	1.30	80.47

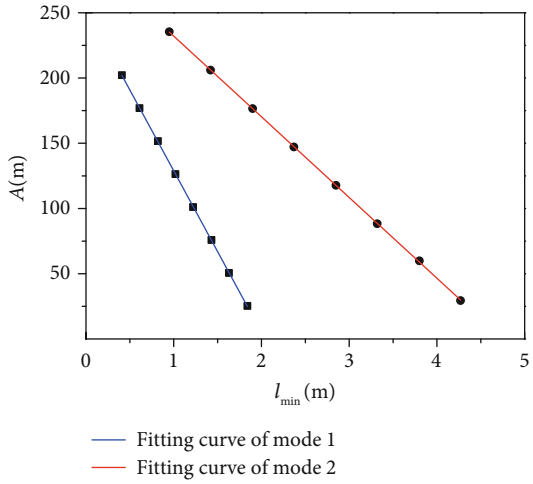

Figure 11: Ratio of the solar collector area to the sewage heat exchanger minimum length in different modes.

principle of the comprehensive evaluation system, indices with a significant influence on the system performance were chosen. The comprehensive evaluation system included three elements—the operating energy consumption, economy and energy saving, and environmental protection—and six targets. The comprehensive evaluation system for the different biogas heating systems is shown in Figure 14.

4.1.1. Operating Energy Consumption Analysis of Different Biogas Heating Systems. To investigate the operating stability of the different biogas heating systems, an operating energy consumption analysis was performed. The EER of the system can be calculated as follows:

$$\mathrm{EER} = \frac{Q_{output}}{Q_{input}}, \tag{11}$$

where EER represents the energy efficiency ratio of the system; Q_{input} represents the input energy of the system,

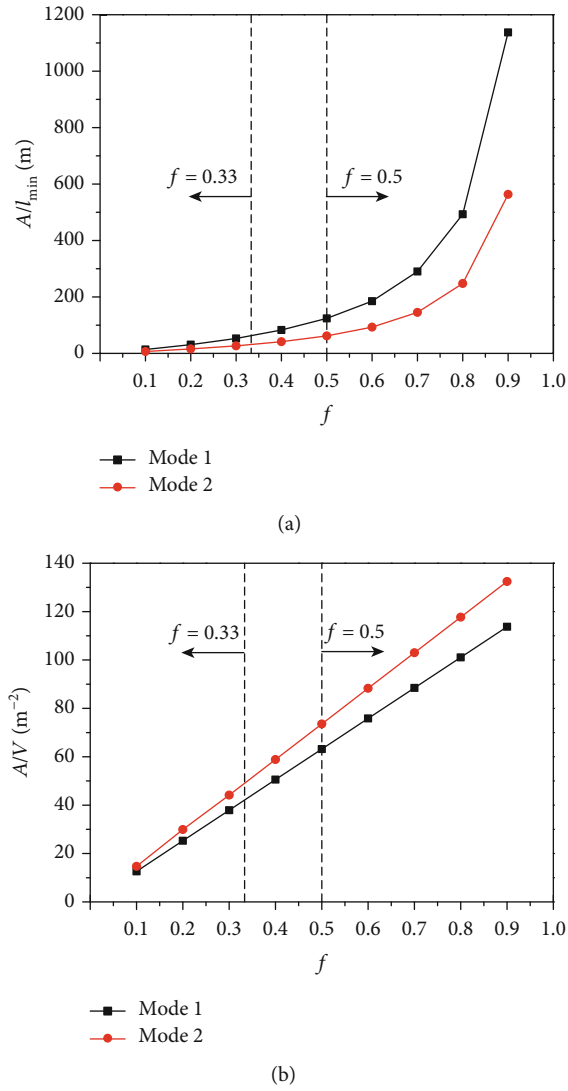

Figure 12: (a) Ratio of the solar collector area to the sewage heat exchanger minimum length with respect to the solar fraction. (b) Ratio of solar collector area to the thermal storage volume with respect to the solar fraction.

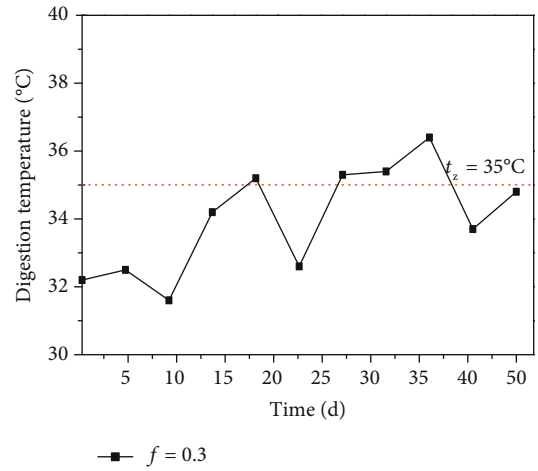

Figure 13: Daily average digestion temperature in the MFD.

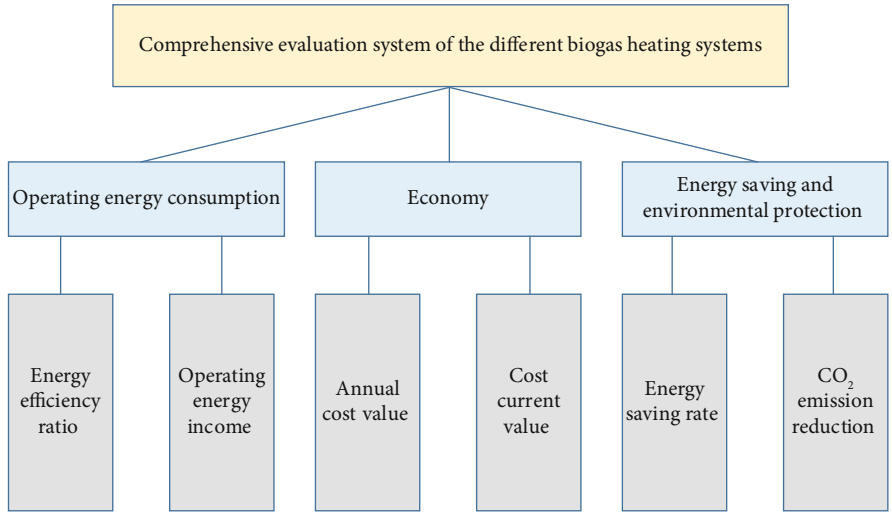

Figure 14: Comprehensive evaluation system for the different biogas heating systems.

Table 7: EER and operating energy income for the different biogas heating systems.

Index	System 1	System 2	System 3	System 4	System 5	Standard deviation
EER	1.01	6.37	3.19	3.19	3.19	1.92
Q_{income} (MJ d^{-1})	1.24	116.06	94.46	94.46	94.46	45.09

including operation energy and heating energy consumption (in MJ d^{-1}); and Q_{output} represents the output energy of the system (in MJ d^{-1}); the value is 137.66 MJ d^{-1} as shown in Reference [19].

The operating energy income quantitatively reflects the operating effectiveness of biogas heating systems and was calculated as follows.

$$Q_{income} = Q_{output} - Q_{input}. \quad (12)$$

Table 7 presents the calculated EER and operating energy income for the different biogas heating systems by Equations (11) and (12). As shown, system 2 had the largest EER and operating energy income, and the EER of system 2 was six times that of system 1. The EER and operating energy income were the same for systems 3, 4, and 5. The operating energy income of systems 3, 4, and 5 was 21.6 MJ d^{-1} smaller than that of system 2, and the EER of these three systems was half that of system 2. The results indicate that system 2 is advantageous with regard to the operating energy consumption.

4.1.2. Economic Analysis of Different Biogas Heating Systems. It was assumed that the systems were operated continuously. Using the annual cost evaluation method, the annual cost value and the cost current value of the different biogas heating systems were calculated as follows:

$$PC = M - N,$$
$$AC = PC\left[\frac{s(1+s)^n}{(1+s)^n - 1}\right] + C + S, \quad (13)$$

where AC represents the annual cost value of the biogas heating system (in yuan); PC represents the present cost value of the biogas heating system (in yuan); M represents the initial investment (in yuan); N represents the net residual value, which was assumed to be 0 yuan; C represents the annual operating cost (in yuan); S represents the annual maintenance cost (in yuan); s represents the annual interest rate of bank deposits (5%–10%); and n represents the service life, which was set as 20 years.

For convenience, the initial investment for the systems was assumed to consist of the equipment cost and installation cost. The initial investment was 2000 yuan kW^{-1} for the heat pump unit, 1200 yuan m^{-1} for the sewage double-pipe heat exchanger, and 200 yuan m^{-2} for the solar collector. The local electricity price was 0.53 yuan kW^{-1} h^{-1}. Accordingly, Table 8 presents the AC and PC values of the different biogas heating systems. As shown, the AC and PC of system 2 were the highest—significantly higher than those of systems 4 and 5—because of the larger solar collector area and higher initial investment for system 2. The AC and PC of systems 4 and 5 were lower than those of system 3, indicating that the use of the sewage double-pipe heat exchanger can effectively reduce the solar-collector cost and improve the system economic performance.

4.1.3. Energy Saving and Environmental Protection Analysis of Different Biogas Heating Systems. For the energy saving and environmental protection analysis of the different biogas heating systems, the energy-saving rate and the CO_2 reduction were considered. Because the primary energy consumption of system 1 was the largest among all the systems, system

Table 8: Economy of the different biogas heating systems.

Index	System 1	System 2	System 3	System 4	System 5	Standard deviation
PC (yuan)	24000	67175.37	52548	6080	18024	25389.21
AC (yuan)	2572.43	7390.96	6013.93	1033.28	2313.49	2699.39

1 was used as the basis for the calculation. The energy-saving rates of the different biogas heating systems were calculated as follows:

$$\eta_i = \left(\frac{H_1 - H_i}{H_1}\right) \times 100\,\% \quad (i = 1, 2, \cdots, 5), H_i = \frac{Q_{\text{input}}}{\eta_a \eta_b}, \tag{14}$$

where η_i represents the energy-saving rate of the biogas heating system relative to system 1 (in %); H_i represents the primary energy consumption of the system (in MJ d^{-1}); η_a represents the generation efficiency, which was set as 35%; and η_b represents the transmission and distribution efficiency, which was set as 90%.

In this study, the small-scale baseline methodology of AMS-I.C, which was approved by the Clean Development Mechanism Executive Board of the United Nations Framework Convention on Climate Change, was used to estimate the system CO_2 emission reductions [33]. The water heating system using conventional fossil fuels was set as a baseline system, which does not consider the CO_2 emission reduction benefits of the biogas power generation and waste heat recovery in later.

$$ER_y = BE_y - PE_y, \tag{15}$$

where ER_y represents the CO_2 emission reduction of the biogas heating system (in kg d^{-1}), BE_y represents the CO_2 emissions of the system under baseline conditions (in kg d^{-1}), and PE_y represents the CO_2 emissions of the system (in kg d^{-1}).

$$\frac{BE_y = 44H_1}{12\eta_n q' \times F_{CO_2}}, \tag{16}$$

where q' is the calorific value of standard coal (29.308 MJ kg^{-1}), F_{CO_2} is the carbon emission factor (0.866), and η_n represents the efficiency of the conventional energy water heating device (95%).

$$PE_y = 0.278 Q_{\text{input}} \times EF_{\text{grid}} + V_i \times \rho_{CO_2}, \tag{17}$$

where EF_{grid} is the power grid emission factor (1.0297 kg CO_2·(kW h)$^{-1}$) [34], V_i represents the CO_2 emission volume of the biogas heating system (in m^3), and ρ_{CO_2} is the density of CO_2 (1.82 kg m^{-3}).

As shown in Table 9, systems 2 and 1 exhibited the best and worst performances, respectively, with regard to the energy-saving rate and CO_2 emission reduction.

4.2. Establishment of Comprehensive Evaluation Model

4.2.1. Improved Entropy Weight Coefficient Method. The mathematical model of the comprehensive evaluation system was constructed according to the improved entropy weight coefficient method [35]. Because of the different units and dimensions of the indices, it was necessary to normalize the indices using the following equation:

$$r_{i,j} = \begin{cases} \dfrac{x_{i,j} - \min\limits_{1 \le i \le n}(x_{i,j})}{\max\limits_{1 \le i \le n}(x_{i,j}) - \min\limits_{1 \le i \le n}} (x_{i,j}) \,(\text{positive indices}), \max\limits_{1 \le i \le n}(x_{i,j}) - x_{i,j} \\ \dfrac{}{\max\limits_{1 \le i \le n}(x_{i,j}) - \min\limits_{1 \le i \le n}(x_{i,j})} \,(\text{negative indices}), \end{cases} \tag{18}$$

where $i = 1, 2, \cdots, n$; $j = 1, 2, \cdots, m$; n is the number of object and m is the number of index; $r_{i,j}$ is the j^{th} index of the i^{th} evaluated system after normalization; and $x_{i,j}$ is the j^{th} index of the i^{th} evaluated system before normalization.

The i^{th} evaluated system index weight $p_{i,j}$ of the j^{th} index is defined as follows:

$$\frac{p_{i,j} = r_{i,j} + 1}{\sum_{i=1}^{n}(r_{i,j} + 1).} \tag{19}$$

The entropy E_j of the j^{th} index is defined as follows:

$$\frac{E_j = -\sum_{i=1}^{n} p_{i,j} \ln p_{i,j}}{\ln n.} \tag{20}$$

The objective weight θ_j of the j^{th} index is defined as follows:

$$\frac{\theta_j = 1 - E_j}{m - \sum_{j=1}^{m} E_j.} \tag{21}$$

The objective weight was improved with the combination of the subjective weight. The subjective weights were determined via the Delphi method. The steps of this method are presented in [36]. The subjective weights were calculated using the MATLAB 2015 software (Table 10) and passed the consistency test ($CR = 0.0417 < 0.1$).

Table 9: Energy-saving rates and CO_2 emission reductions of the different biogas heating systems.

Index	System 1	System 2	System 3	System 4	System 5	Standard deviation
η_i (%)	0	62.61	25.22	25.22	25.22	22.39
ER_y (kg d^{-1})	5.56	14.73	8.55	8.55	8.55	3.36

The synthetic weight γ_j of the j^{th} index is defined as follows:

$$\gamma_j = \frac{\theta_j w_j}{\sum_{j=1}^{m} \theta_j w_j}. \quad (22)$$

The comprehensive evaluation value λ_i of the i^{th} evaluated system was calculated as follows:

$$\lambda_i = \sum_{j=1}^{m} \gamma_j p_{i,j}. \quad (23)$$

Figure 15 presents the comprehensive evaluation values of the different biogas heating systems. As shown in Table 10, the EER and *PC* had the largest synthetic weight, and the energy-saving rate had the smallest synthetic weight. The comprehensive evaluation values of the systems decreased in the following order: System 4 > System 5 > System 2 > System 3 > System 1. System 4 had the largest comprehensive evaluation value of 0.2251. Although systems 4 and 5 were not optimal with regard to the EER, system operating energy income, energy-saving rate, and CO_2 emission reduction, they were excellent with regard to the system economic performance, particularly the initial investment.

4.2.2. Delphi-Variation Coefficient Combination Weighting Method. The mathematical model of the comprehensive evaluation system was based on the Delphi-variation coefficient combination weighting method [37]. The matrix of normalized indices $\mathbf{R}_{i,j}$ was constructed using Equation (18).

The variation coefficient is defined as follows:

$$v_j = \frac{\sigma_j}{\overline{x_j}}, \quad (24)$$

where $j = 1, 2, \cdots, m$; v_j is the variation coefficient of the j^{th} index; σ_i represents the standard deviation of the j^{th} index; and $\bar{x}$ represents the average value of the j^{th} index.

By normalizing Equation (24), the objective weight θ_j of the j^{th} index can be described as follows:

$$a_j = \frac{v_j}{\sum_{j=1}^{m} v_j}. \quad (25)$$

The synthetic weight is defined as follows:

$$\tau_j = \lambda w_j + (1 - \lambda) a_j, \quad (26)$$

Table 10: Entropy and weight of each index.

Index	E_j	θ_j	w_j	γ_j
EER	0.9851	0.1504	0.2431	0.2175
Q_{income} (MJ d^{-1})	0.9849	0.1520	0.1231	0.1113
PC (yuan)	0.9814	0.1876	0.2689	0.3001
AC (yuan)	0.9806	0.1952	0.1328	0.1542
η_i (%)	0.9850	0.1508	0.1196	0.1073
ER_y (kg d^{-1})	0.9837	0.1639	0.1125	0.1097
Standard deviation	0.001981	0.01996	0.06998	0.07795

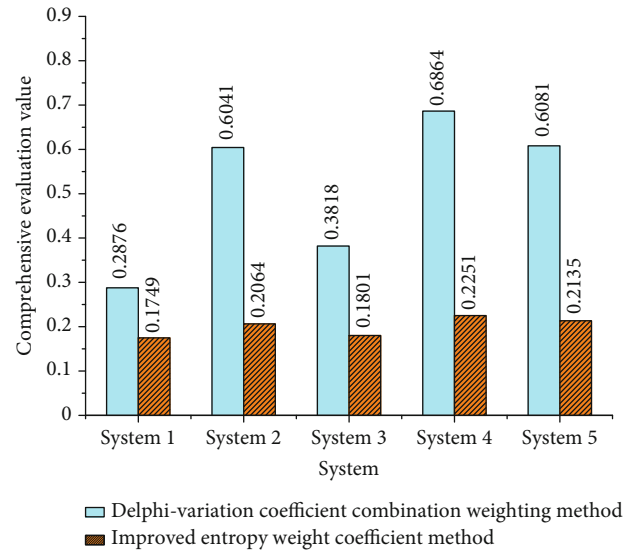

Figure 15: Comprehensive evaluation values of the different biogas heating systems.

where τj is the synthetic weight of the j^{th} index, and λ is the preference coefficient, which was set as 0.6.

Finally, the comprehensive evaluation value b_i of the i^{th} evaluated system was given as follows:

$$b_i = \sum_{j=1}^{m} \tau_j r_{i,j}. \quad (27)$$

As shown in Table 11 and Figure 15, the EER and *PC* had the largest impact on the comprehensive evaluation value of the system, and the energy-saving rate had the smallest impact. As shown in Figure 15, the standard deviation is 0.1699 for Delphi-variation coefficient weighting method and is 0.1851 for improved entropy weight coefficient

Table 11: The variation coefficient and weight of each index.

Index	v_j	a_j	w_j	τ_j
EER	0.5059	0.1505	0.2431	0.2175
Q_{income} (MJ d^{-1})	0.5032	0.1497	0.1231	0.1113
PC (yuan)	0.6766	0.2013	0.2689	0.3001
AC (yuan)	0.6247	0.1859	0.1328	0.1542
η_i (%)	0.7240	0.2154	0.1196	0.1073
ER_y (kg d^{-1})	0.3269	0.0972	0.1125	0.1097
Standard deviation	0.1450	0.04317	0.06998	0.07795

method; the system rankings obtained via the two methods were the same. The comprehensive evaluation values of the systems decreased in the following order: System 4 > System 5 > System 2 > System 3 > System 1. System 4 had the largest comprehensive evaluation value of 0.6864.

4.3. Kendall's W Test. Different evaluation methods may have different results. Therefore, to investigate whether the conclusions of the two comprehensive evaluation methods were consistent, Kendall's W coefficient test was conducted [38]. And the coefficient is defined as follows:

$$R_i = \sum_{j=1}^{m} r_{i,j},$$
$$W = \frac{12\sum_{i=1}^{n} R_i^2 - 3b^2 n(n+1)^2}{b^2 n(n^2-1)}, \quad (28)$$

where R_i is the rank of the i^{th} evaluated system; b is the number of comprehensive evaluation method.

Moreover, using the SPSS software, the evaluation results of the two comprehensive evaluation methods were compared according to Kendall's W coefficients. The results were Kendall's $W = 0$ and saliency Asymp.Sig. = 1.000, indicating that the evaluation results of the two methods were in good agreement. Therefore, the SUSSHPS was the optimal system among the four heating systems. When the untreated sewage is sufficient, system 4 can be used directly. Conversely, if the untreated sewage is insufficient ($l_{min} \le l \le l_{max}$), solar energy can be used for supplementation. In general, more factors must be taken into account, such as the sewage flow, the construction conditions and difficulty of the sewage double-pipe heat exchanger, and the sewage temperature. The values of the solar collector area and the length of the sewage double-pipe heat exchanger can be defined according to the principle of the maximization of system benefits.

5. Conclusion

For improving the conventional biogas heating system, this paper proposed an SUSSHPS for the MFD dynamic anaerobic digestion system. Two operating modes were defined according to the solar fractions in different regions: mode 1 for general-solar energy resource areas and mode 2 for solar energy resource-rich areas. Based on the thermodynamic calculations and experiments study, the parameters of A_c and l_{min} for the two modes were calculated. And we also clear the suitable conditions of the two modes.

Furthermore, to examine the advantages of the SUSSHPS, a comprehensive evaluation of a biogas boiler heating system, a solar direct heating system, a solar source heat pump heating system, and the SUSSHPS ($l = l_{min}$ and $l = l_{max}$) was performed. According to the experimental data and calculated values, a comprehensive evaluation system was constructed, which consisted of three elements and six indices. Moreover, a mathematical model of the comprehensive evaluation system was constructed via the improved entropy weight coefficient method and the Delphi-variation coefficient combination weighting method. The results of the two methods were the same. The biogas boiler heating system and the SUSSHPS exhibited the smallest and largest comprehensive evaluation values, respectively. It is indicated that the SUSSHPS was the optimal system among the four heating systems, exhibiting excellent system economic performance, as well as outstanding energy saving and environmental protection. However, many other factors should be considered, such as the sewage flow and sewage temperature, and the maximization of the system benefits should be the guiding principle in the practical application of the proposed system.

Nomenclature

EER: Energy efficiency ratio
COP: Coefficient of performance
TS: Total solid concentration of fermentation slurry (%)
VS: Volatile solid concentration of fermentation slurry (%)
COD: Chemical oxygen demand (g L^{-1})
BOD_5: Biochemical oxygen demand (g L^{-1})
Q_{demand}: Heat duty of the dynamic anaerobic digestion system (kW)
Q_1: Heat required for heating the biomass digestive fluid (kW)
Q_2: Heat loss from the MFD and slurry tank (kW)
T_{hot}: Temperature of the hot source (K)
T_{cold}: Temperature of the cold source (K)
$Q_{storage}$: Heat required for heat storage tank (kW)
Q_{solar}: Heat supplied by solar collector (kW)
Q_{sewage}: Heat supplied by untreated sewage (kW)
W: Heat supplied by heat pump unit (kW)
f: Solar fraction (%)
l_{min}: Minimum length of the sewage double-pipe heat exchanger (m)
t_{sewage}: The calculation temperature of the sewage in winter (K)
t_{in}: Average inlet temperatures of the chilled water (K)
t_{out}: Average outlet temperatures of the chilled water (K)
k_m: Heat transfer coefficient of the heat exchanger (W m^{-1} K^{-1})
R_I: Fouling resistance (m K W^{-1})
h_0: Convection heat transfer coefficient of the inner pipe internal surface (W m^{-2} K^{-1})

r_i: Inner pipe radius of the sewage double-pipe heat exchanger (m)
r_0: Outer pipe radius of the double-pipe heat exchanger (m)
δ_i: Thickness of the inner pipe wall (m)
δ_0: Thickness of the outer pipe wall (m)
Nu: Nusselt criterion number
λ_0: Heat conductivity coefficient of the chilled water ($W\,m^{-1}\,K^{-1}$)
D_e: Characteristic length of the sewage double-pipe heat exchanger (m)
A_c: Area of the direct system (m^2)
J_T: Average daily amount of solar radiation ($MJ\,m^{-2}\,d^{-1}$)
η_g: Average heat loss rate of the solar collector (%)
η_d: Average collection efficiency of the solar collector (%)
η_s: Heat loss efficiency of the direct system (%)
Q_c: Heat duty of the solar collector ($MJ\,d^{-1}$)
Q_{input}: Input energy of the system ($MJ\,d^{-1}$)
Q_{output}: Output energy of the system ($MJ\,d^{-1}$)
Q_{income}: Energy income of the system ($MJ\,d^{-1}$)
PC: Cost current value of the biogas heating system (yuan)
AC: Annual cost value of the biogas heating system (yuan)
M: Initial investment (yuan)
N: Net residual value (yuan)
C: Annual operating cost (yuan)
S: Annual maintenance cost (yuan)
s: Annual interest rate of bank deposits (%)
n: Service life (year)
H_i: Primary energy consumption of the system ($MJ\,d^{-1}$)
η_i: Energy-saving rate of the biogas heating system relative to system 1 (%)
η_a: Generation efficiency (%)
η_b: Transmission and distribution efficiency (%)
ER_y: CO_2 emission reduction of the biogas heating system ($kg\,d^{-1}$)
BE_y: CO_2 emissions of the system under baseline conditions ($kg\,d^{-1}$)
PE_y: CO_2 emissions of the system ($kg\,d^{-1}$)
q': Calorific value of standard coal ($MJ\,kg^{-1}$)
F_{CO_2}: CO_2 emission factor (%)
V_i: CO_2 emission volume of the biogas heating system (m^3)
EF_{grid}: Power grid emission factor ($kg\,CO_2\cdot(kW\,h)^{-1}$)
ρ_{CO_2}: Density of CO_2 ($kg\,m^{-3}$).

Abbreviations

SUSSHPS: Solar-untreated sewage source heat pump system
MFD: Multiphase flow digester.

Data Availability

The data used to support the findings of this study are included within the article.

Conflicts of Interest

The authors declare that they have no conflicts of interest.

Acknowledgments

Financial supports from the National Natural Sciences Foundation of China (No. 51378426), the Sichuan Province Youth Science and Technology Innovation Team of Building Environment and Energy Efficiency (No. 2015TD0015), and the Sichuan Province Science and Technology Support Program (No. 2016JZ0018) are sincerely acknowledged.

References

[1] A. Aslani, T. Mazzuca-Sobczuk, S. Eivazi, and K. Bekhrad, "Analysis of bioenergy technologies development based on life cycle and adaptation trends," *Renewable Energy*, vol. 127, pp. 1076–1086, 2018.

[2] T. M. Alkhamis, R. El-khazali, M. M. Kablan, and M. A. Alhusein, "Heating of a biogas reactor using a solar energy system with temperature control unit," *Solar Energy*, vol. 69, no. 3, pp. 239–247, 2000.

[3] K. Rajendran, S. Aslanzadeh, and M. J. Taherzadeh, "Household biogas digesters – a review," *Energies*, vol. 5, no. 8, pp. 2911–2942, 2012.

[4] N. Krakat, A. Westphal, S. Schmidt, and P. Scherer, "Anaerobic digestion of renewable biomass: thermophilic temperature governs methanogen population dynamics," *Applied and Environmental Microbiology*, vol. 76, no. 6, pp. 1842–1850, 2010.

[5] J. Lundgren, R. Hermansson, and J. Dahl, "Experimental studies of a biomass boiler suitable for small district heating systems," *Biomass and Bioenergy*, vol. 26, no. 5, pp. 443–453, 2004.

[6] T. Zhang, Y. Tan, and X. Zhang, "Using a hybrid heating system to increase the biogas production of household digesters in cold areas of China: an experimental study," *Applied Thermal Engineering*, vol. 103, pp. 1299–1311, 2016.

[7] R. Feng, J. Li, T. Dong, and X. Li, "Performance of a novel household solar heating thermostatic biogas system," *Applied Thermal Engineering*, vol. 96, pp. 519–526, 2016.

[8] A. A. M. Hassanein, L. Qiu, P. Junting, G. Yihong, F. Witarsa, and A. A. Hassanain, "Simulation and validation of a model for heating underground biogas digesters by solar energy," *Ecological Engineering*, vol. 82, pp. 336–344, 2015.

[9] H. Shi, T. Wang, H. Zhu, Y. Li, L. Rong, and X. Pei, "Heating system of biogas digester by ground-source heat pump," *Transactions of the Chinese Society of Agricultural Engineering*, vol. 26, pp. 268–273, 2010.

[10] J. Liu, W. Li, Z. Chen, and W. Sha, "Heating mode of biogas plant in alpine region based on underground water source heat pump," *Transactions of the Chinese Society of Agricultural Engineering*, vol. 29, pp. 163–169, 2013.

[11] S. Tiwari, J. Bhatti, G. N. Tiwari, and I. M. al-Helal, "Thermal modelling of photovoltaic thermal (PVT) integrated greenhouse system for biogas heating," *Solar Energy*, vol. 136, pp. 639–649, 2016.

[12] N. Curry and P. Pillay, "Integrating solar energy into an urban small-scale anaerobic digester for improved performance," *Renewable Energy*, vol. 83, pp. 280–293, 2015.

[13] S.-J. Cao, X.-R. Kong, Y. Deng, W. Zhang, L. Yang, and Z.-P. Ye, "Investigation on thermal performance of steel heat exchanger for ground source heat pump systems using full-scale experiments and numerical simulations," *Applied Thermal Engineering*, vol. 115, pp. 91–98, 2017.

[14] G. D. Qin, P. Lou, and X. L. Wu, "Study on warming parallel system with solar energy, air source heat pump and electric heat of biogas fermentation," *Transactions of The Chinese Society of Agricultural Machinery*, vol. 35, pp. 187–194, 2014.

[15] P. Guo, R. J. Ma, and N. Y. Yu, "Operation mode of solar and untreated sewage source heat pump system for heating biogas digester," *Journal of Southwest Jiaotong University*, vol. 53, pp. 1087–1094, 2018.

[16] X. M. Pei, H. X. S. Di Zhang, H. G. Zhu, Y. Lei, and Z. Wang, "Collector area optimization of integrated solar and ground source heat pump system for heating biogas digester," *Nongye Jixie Xuebao= Transactions of the Chinese Society for Agricultural Machinery*, vol. 42, pp. 122–128, 2011.

[17] H. X. Shi, D. T. Xu, H. G. Zhu, Y. L. Zhang, X. Z. Meng, and C. C. Guo, "TRNSYS simulation of integrated solar and ground source heat pump for biogas digester heating system," *Transactions of The Chinese Society of Agricultural Machinery*, vol. 48, pp. 288–295, 2017.

[18] J. Kim, H.-J. Choi, and K. C. Kim, "A combined dual hot-gas bypass defrosting method with accumulator heater for an air-to-air heat pump in cold region," *Applied Energy*, vol. 147, pp. 344–352, 2015.

[19] P. Guo, J. Zhou, R. Ma, N. Yu, and Y. Yuan, "Biogas production and heat transfer performance of a multiphase flow digester," *Energies*, vol. 12, no. 10, p. 1960, 2019.

[20] Y. Liu, Y. Chen, Y. Zhou, D. Wang, Y. Wang, and D. Wang, "Experimental research on the thermal performance of PEX helical coil pipes for heating the biogas digester," *Applied Thermal Engineering*, vol. 147, pp. 167–176, 2019.

[21] F. Dong and J. Lu, "Using solar energy to enhance biogas production from livestock residue - A case study of the Tongren biogas engineering pig farm in South China," *Energy*, vol. 57, pp. 759–765, 2013.

[22] A. C. Yiannopoulos, I. D. Manariotis, and C. V. Chrysikopoulos, "Design and analysis of a solar reactor for anaerobic wastewater treatment," *Bioresource Technology*, vol. 99, no. 16, pp. 7742–7749, 2008.

[23] Y. C. Zhong, Z. F. Ma, J. X. Xu, and H. Y. Guo, "Assessment of solar energy resource in Sichuan based on distributed modeling on rugged terrains," *Journal of Southwest University (Natural Science Edition)*, vol. 40, pp. 115–121, 2018.

[24] Y. Lu, Y. Tian, H. Lu, L. Wu, and X. Li, "Study of solar heated biogas fermentation system with a phase change thermal storage device," *Applied Thermal Engineering*, vol. 88, pp. 418–424, 2015.

[25] X. D. Wang, L. Zhao, and Y. H. Li, "Operating performance analysis on heating conditions of sewage source heat pumps," *HV&AC*, vol. 38, pp. 99–102, 2008.

[26] X. Zhang, Z. Ren, and F. Mei, *Heat Transfer*, China Architecture & Building Press, Beijing, China, 5th edition, 2007.

[27] Z. Liu, L. Ma, and J. Zhang, "Application of a heat pump system using untreated urban sewage as a heat source," *Applied Thermal Engineering*, vol. 62, no. 2, pp. 747–757, 2014.

[28] Z. N. He and D. Z. Zhu, *Solar Heating Application Manual*, Chemical Industry Press, Beijing, China, 2009.

[29] L. Zhang, W. Du, J. Wu, Y. Li, and Y. Xing, "Fluid flow characteristics for shell side of double-pipe heat exchanger with helical fins and pin fins," *Experimental Thermal & Fluid Science*, vol. 36, pp. 30–43, 2012.

[30] M. Villa-Arrieta and A. Sumper, "A model for an economic evaluation of energy systems using TRNSYS," *Applied Energy*, vol. 215, pp. 765–777, 2018.

[31] S. B. Xu, D. S. Xu, and L. L. Liu, "Construction of regional informatization ecological environment based on the entropy weight modified AHP hierarchy model," *Sustainable Computing: Informatics and Systems*, vol. 22, pp. 26–31, 2019.

[32] Z. Wang, M. Song, F. Wang, Z. Ma, and Q. Lin, "Experimental investigation and seasonal performance assessment of a frost-free ASHP system with radiant floor heating," *Energy and Buildings*, vol. 179, pp. 200–212, 2018.

[33] "Consolidated baseline methodology for GHG emission reductions from manure management systems (ACM0010)," http://cdm.unfccc.int/methodologies/PAmethodologies/approved.html.

[34] Y. E. Li, H. Dong, Y. Wan, X. Qin, Q. Gao, and L. Hua, "Emission reduction from clean development mechanism projects on intensive livestock farms and its economic benefits," *Transactions of the Chinese Society of Agricultural Engineering*, vol. 25, pp. 194–198, 2009.

[35] H. Xu, C. Ma, J. Lian, K. Xu, and E. Chaima, "Urban flooding risk assessment based on an integrated k-means cluster algorithm and improved entropy weight method in the region of Haikou, China," *Journal of Hydrology*, vol. 563, pp. 975–986, 2018.

[36] B. Sun, J. Jiang, F. Zheng et al., "Practical state of health estimation of power batteries based on Delphi method and grey relational grade analysis," *Journal of Power Sources*, vol. 282, pp. 146–157, 2015.

[37] G. Y. Wang, *Civil engineering's comprehensive evaluation technology and application*, China Water Conservancy and Electricity Press, Beijing, China, 2011.

[38] W. Zhang, J. Lu, and Y. Zhang, "Comprehensive evaluation index system of low carbon road transport based on fuzzy evaluation method," *Procedia Engineering*, vol. 137, pp. 659–668, 2016.